Barium ferrite and its Possible Applications

Majahid Ul Islam, Shahnaz Kossar, Raj Paul

Introduction

Materials science has shaped the development of civilizations since the dawn of mankind. With the development of materials science, the driving development and economic growth are the main factors [1]. During 1950s, the material science research based on silicon industrial revolution have radically impacted and transformed our society by enabling the emergence of the todays technologies [2]. Such as wireless communications, mobile phones, digital data storage and widespread consumer electronics [3,4,5]. Today's emergent topics in material science and technology includes nano-materials[ref 6], spintronic materials[Ref7], bio-materials [8,9], carbon nano-tubes, graphene , multiferroic materials[11], smart and advanced functional materials, which promise to deliver a new wave of technological advances as compare to the silicon industrial revolution. Over the past 15 years, multiferroic materials have become increasingly popular due to their interesting physical, chemical properties and high potential for technological applications [12,13].

Multiferroic materials are the type of solid-state compounds that possesses more than one order of states such as ferromagnetism, ferroelectricity, ferroelasticity, and ferrotoroidicity with in one phase [14,15,16]. Such types of multiferroics were able to display the strong piezo-electric, piezo-magnetic as well as magneto-elastic and electro-elastic properties [17]. Both of these materials (ferromagnetic and ferroelectric) are essential for technological applications, because they are able to control both ferroelectric and ferromagnetic properties via external mechanical stress due to the coupling between the phases [18,19,20]. Furthermore, the converse effects which is externally applied for magnetic and electric fields to modify the shape of the material by introducing a mechanical strain . This complex coupling between magnetization - magnetic field – strain, electric polarization-electric field-strain, and stress - strain - electric polarization - magnetization is graphically illustrated in figure 1.

The coexistence of ferro-order and piezo-elastic property es can produce interesting piezo-electric and piezo-magnetic couplings. It important to note that by electric and magnetic order state, any sort of ferroic order is observed, including ferromagnetic, anti-ferromagnetic,

ferri-magnetic,and paramagnetic orders, as well as their electrical equivalents, if applicable. However,what fascinates scientists about multiferroic materials is not just their ability to exhibit numerous order states, but also the cross-coupling effects that can occur between the order states.

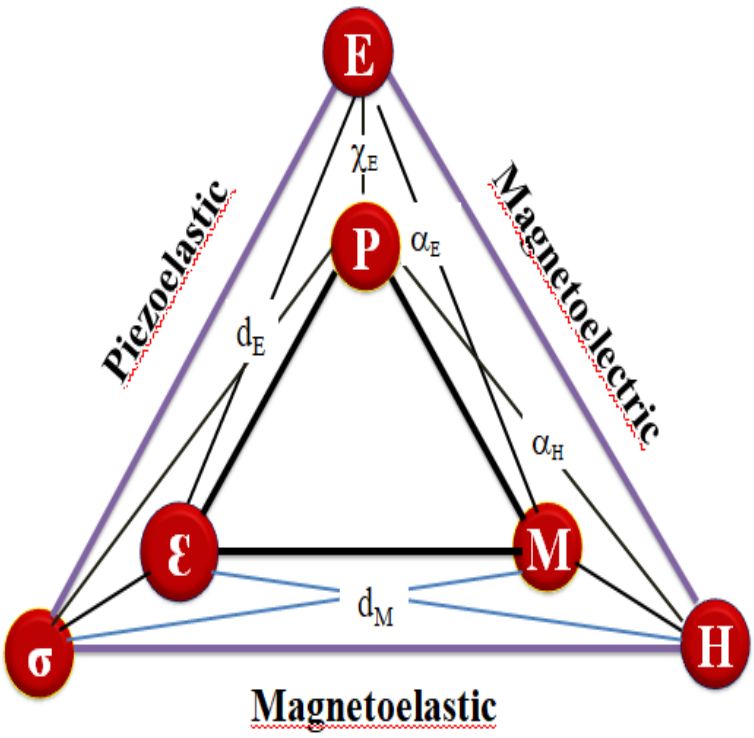

Figure 1. Coupling electric-elastic-magnetic properties in multiferroic showing order parameters and conjugate fields E – electric field; σ - applied mechanical stress;; H – magnetic field, P – electric polarization; M – magnetization and ε - strain.

Hysteresis loops, which show the maximum magnetization/polarization with applied magnetic/electric fields, coercive magnetic/electric fields, and remanent magnetization/polarization, etc., are used to describe ferroelectric and ferrromagnetic materials. Figure 2 shows the common spin and dipole configurations and hysteresis loops in ferroelectric and ferromagnetic materials[21].

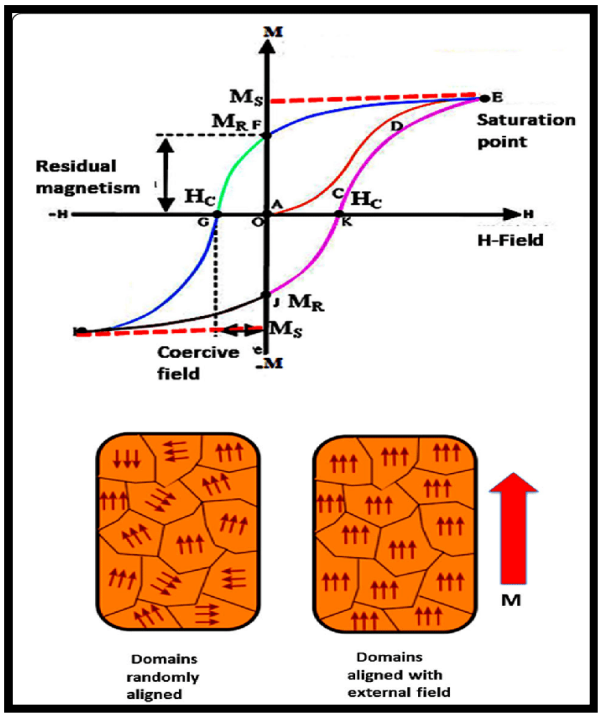

Figure 2 Ferroelectric and ferromagnetic hysteresis loop and ordering of spins (left) and dipoles (right); M : Magnetization, H :Magnetic field, P : Electric polarization and E : Electric field [22].

Many ferroelectric and ferromagnetic materials have been reported in the literature, and they are now an important component of modern science and technology. For instance, ferroelectric material exhibiting electric-field-induced switchable, spontaneous electric polarizations have been used in non-volatile ferroelectric memories. Similarly magnetic data storage devices and magnetic read-and-write heads of electronic devices have both been made of ferromagnetic materials.The coexistence of ferroelectricity and ferromagnetism in multiferrites makes them extremely appealing for a variety of technological applications. For example, these materials are used in spintronics, where the manipulation of electron charge and spin is critical, Multiferrites can be used to make new memory devices, sensors, actuators, energy harvesting devices and also in biomedical applications[23]. Bismuth ferrite (BiFeO3), bismuth manganite (BiMnO3), barium nitrate(BaTiO3) , Barium ferrite (BaFeO3), and yttrium iron garnet ($Y_3Fe_5O_{12}$) are all examples of multiferrite minerals. Because of their multifunctional features and possible applications, these materials have attracted the curiosity of researchers. In this chapter we will focus on stracture and some of the best application of M type hexagonal ferritrs.

2 Stracture and properties of Hexagonal Multiferrites

The magnetic mineral magnetoplumbite was initially described in 1925 [24], and in 1938 the crystal structure was determined to be hexagonal with the composition $PbFe_{7.5}Mn_{3.5}Al_{0.5}Ti_{0.5}O_{19}$ [25]. The synthetic form of magnetoplumbite was discovered to be $PbFe_{12}O_{19}$, or pure PbM and a number of isomorphous compounds were proposed, including $BaFe_{12}O_{19}$. Jonker, Wijn, and Braun also found other compounds when the ternary $BaO\text{-}Fe_2O_3\text{-}MeO$ system was heated to 1200–1400 °C[26,27]. There are numerous types of hexagonal ferrites, sometimes known as hexaferrites. These hexaferrites are: M-type ferrites-Barium ferrite or BaM ($BaFe_{12}O_{19}$); W-type ferrites $BaCo_2Fe_{16}O_{27}$ Such as Fe_2W ($BaFe_2Fe_{16}O_{27}$); X-type ferrites $Ba_2Me_2Fe_{28}O_{46}$, such as Co_2X ($Ba_2Co_2Fe_{28}O_{46}$); Y-type ferrites $Ba2\ Me_2Fe_{12}O_{22}$, such as Co_2Y ($Ba_2Co_2Fe_{12}O_{22}$); U-type ferrites $Ba4Me2Fe_{36}O_{60}$, such as Co_2U ($BaCo_2Fe_{36}O_{60}$) and Z type ferrites-$Ba_2Me_2Fe_{24}O_{41}$, Such as Co_2Z ($Ba_2Co_2Fe_{24}O_{41}$). Where, “Me” is a divalent first row transition metal or some other divalent cation.[28].All of these compounds were discovered to have a hexagonal crystal structure, with two crystalline lattice parameters: a, the width of the hexagonal plane, and c, the crystal height.

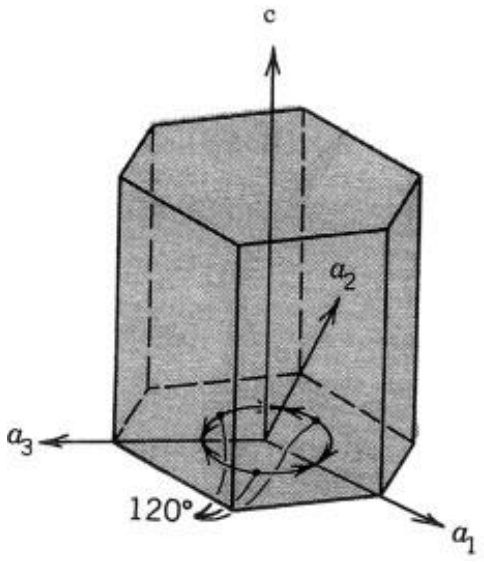

Figure 3: Hexagonal crystal, showing the two lattice parameters a and c. Adoped from [29]

The physical characteristics of different types of hexaferrite is shown in the table .

Ferrites (Type)	Formulla	Molecular mass(g)	Density ρ (g/ cm)	c (Å)	Magnetisation (at room temperature)
BaM	$BaFe_{12}O_{19}$	1112	5.29	23.18	Uniaxial
SrM	$SrFe_{12}O_{19}$	1062	5.11	23.02	Uniaxial
Co_2W	$BaCo_2Fe_{16}O_{27}$	1577	5.31	32.84	In cone
Co_2X	$Ba_2Co_2Fe_{28}O_{46}$	2688	5.29	84.11	In Cone
Co_2Y	$Ba_2Co_2Fe_{12}O_{22}$	1410	5.40	4356	In plane
Co_2Z	$Ba_2Co_2Fe_{24}O_{41}$	2522	5.35	52.30	In plane
Co_2U	$BaCo_2Fe_{36}O_{60}$	3624	5.31	3816	In plane

Table 1: Some physical characteristics of the hexagonal ferrites at room temperature[29].

M-type hexaferrites

Barium ferrite (BaM)

The compound BaM, $BaFe_{12}O_{19}$, were studied for the first time in the 1936 with a melting point of 1390 °C [30]. However, the structure was not established as being isomorphous with the hexagonal magnetoplumbite until Philips examined and defined it magnetically in the early 1950s [29]. These ferrites had lower saturation magnetisation than conventional alloy magnets, were significantly cheaper to manufacture, had a high electrical resistance of 10^8 Ohm cm, and a high magnetic uniaxial anisotropy(~17 kOe) along the c-axis. BaM has a molecular mass of 1112 g Mol^{-1} and a maximum density of 5.295 g /cm^3 [31], but in practise, the ceramic material frequently has a density as low as 90% of its theoretical density. BaM's c-axis hardness has been estimated to be 5.9 GPa [32].

The hexagonal crystal structure of BFO with the space group P 63/mmc. is shown in figure 4[33,34]. This structure can be represented symbolically as RSR*S, where R denotes a three layer block having two O_4 and one BaO_3 with the composition Ba^{2+} $Fe_6^{3+}O_{11}^{2-}$, and S signifies a two layer block containing two O_4 with the composition $Fe_6^{3+}O_8^{2-}$. The asterisk indicates a 180-degree rotation of the corresponding block about the c-axis. Moitra et al achieved a = 5.35 A and c = 21.19 A as the equilibrium lattice constants of the hexagonal unit cell by optimising the volume and shape of the unit cell and the internal coordinates, which are in good agreement with the experimental values of 5.90 A and 23.24 A, respectively [35].

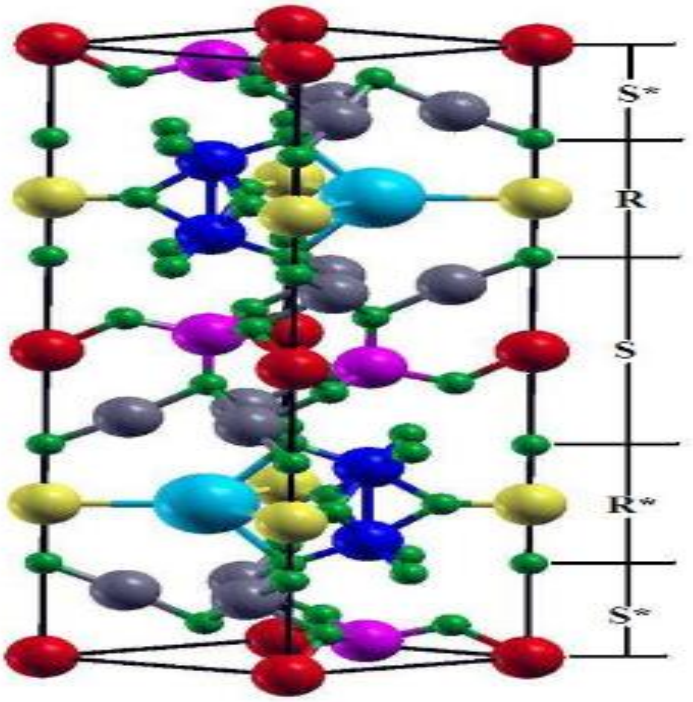

Figure 4: Crystal structure of M-type barium hexaferrite. Red, gray, pink, blue and yellow colored spheres represent iron atoms in 2a, 12k, 4f1, 4f2, and 2b sites respectively. Green spheres represent oxygen atoms, while larger cyan spheres represent barium atoms.[35]

Strontium M-type hexagonal ferrite (SrM)

Strontium M-type hexagonal ferrite (SrM) discovered by Cockherdt in 1963[36] , is a ferrite that belongs to the magnetoplumbite phase [29]. Due to the comparatively strong magnetocrystalline anisotropy field, the $SrFe_{12}O_{19}$ ferrimagnet displays extraordinary magnetic properties of saturation magnetization (70 emu/g) and coercivity (6.64 kOe) [37,38,39].The availability and quantity of raw materials, the comparatively low cost of manufacturing, the outstanding chemical stability and anticorrosion capabilities, and the relatively high Curie temperature (470 °C) are all advantages[40].

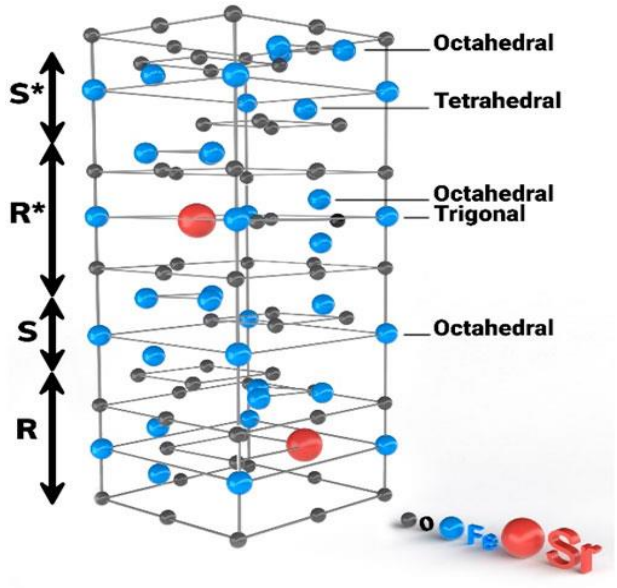

Figure 4: Unit cell of SrM (contain S block and R block) adopted from [43].

SrM has a hexagonal structure with a space group of P63/mmc and is made up of four blocks (RSR*S*), where S is spinal =$Fe_6O_8^{2+}$ and R is hexagonal =$MFe_6O_{11}^{2-}$ are the main elements [41,42]. The asterisk (*) denotes that the subunit has been rotated 180 degrees around the crystallographic c-axis. The total magnetization of the unit cell at absolute zero temperature is proportional to the number of Fe^{3+} ions.

There is an equal distribution of Fe^{3+} ions between the two blocks. In the hexagonal structure of the R block, five ions are arranged in an octahedral pattern with three spins up, two spins down the magnetic moments, and one spin up the magnetic moment on the bipyramidal site. The S block with spinel stracture contains four of the six Fe^{3+} ions in the octahedral position. The octahedral cations have spin-up moments, while the two ions at the tetrahedral positions have spin-down moments. Three or more ions are distributed equally across the two blocks.

Due to these exceptional qualities, $SrFe_{12}O_{19}$ has found widespread use in a variety of technological applications, including magneto-optic systems, power electronics, transformer core, electric motors, the telecommunications industry, automotive parts, microwave absorbers, magnetic recording media, memory devices and sensors. [44,45,46,47,48].

Lead M-type hexagonal ferrite (PbM)

In M type hexaferrite family, lead ferrite is hard magnetic material with low synthesis and sintering temperatures. PbM has a molecular mass of 1181g, Which is much heavier than barium and strontium and a density of 5.708 g /cm^3[49].The Pb2+ ion size lies in between the barium and Strontium. Figure 1a depicts the structure of $PbFe_{12}O_{19}$. It is composed of spinel and hexagonal blocks, similar to other hexaferrites with magnetoplumbite structures. Along the c axis, oxygen anions and large lead ions are densely packed an alternation sequence of 10 ABABACBCBC layers, where the third and eighth layers contain Pb2+ cations. One unit cell

includes two PbFe12O19 formula units. Pb^{2+} cations have an anticuboctahedral first oxygen coordination sphere (Figure 1b), whereas iron cations have five nonequivalent crystallographic positions (Figure 1c-g): Fe_1 (2a), Fe4 (4f1), and Fe5 (12k) and have an octahedral, Fe2 (2b), and Fe3 (4f2), respectively, trigonal-bipyramidal, and tetrahedral

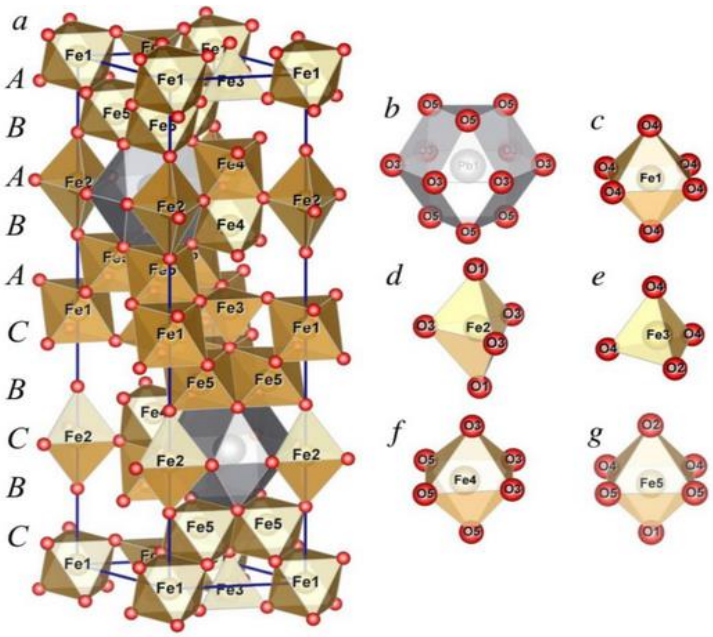

Figure 5. The unit cell of $PbFe_{12}O_{19}$ (**a**) and the coordination polyhedra of the cations Pb^{2+} (**b**) and Fe^{3+} (**c**–**g**) adopted from [50]

Table 2. Some physical and thermal values and properties of BaM, SrM and PbM ferrites. d = density in g/cm^3[11]. T_m = melting point in Kelvin ,αa , αc and αv = average thermal expansion coefficients for a axis, c axis and volume, in 10 ^{6}/ K. a and c = lattice parameters. v = cell volume and Tc = Curie temperature, in K [29].

	δ	T_m	α_a	α_c	α_v	a	c	V	T_c
SrM	5.101	1692	8.62	16.08	33.50	5.8844	23.0632	691.6	732
BaM	5.295	1611	10.74	16.29	38.16	5.8876	23.1885	696.2	725
PbM	5.708	1538	10.80	18.34	40.46	5.8941	23.0984	694.9	718

Applications of M ferrites

M-type hexaferrite and related compounds have many applications due to their exceptional electric and magnetic properties. Some of the main application of M type hexaferrites are microwave absorber, magnetic recording, biomedical application like hyperthermia (cancer treatment) and high frequency electronic devices .

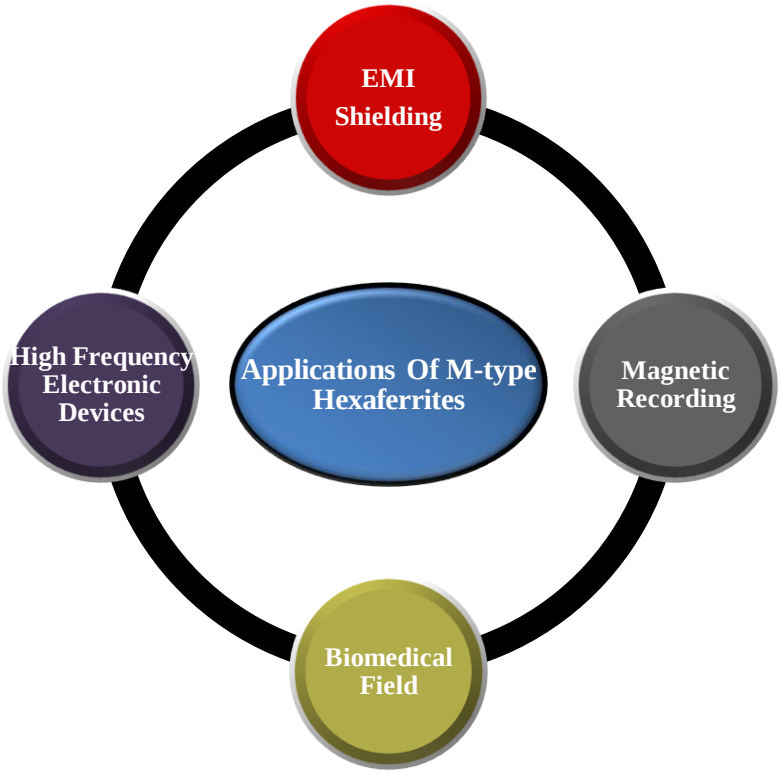

Figure 6: shows the some application of M-type hexaferrites.

1. **Electromagnetic Interference (EMI) Shielding.**

For the uninterrupted operation of electronic equipment, the absence of electromagnetic interference in these devices is crucial. This is achieved by using materials that would absorb electromagnetic radiations that are primary as well as secondary [51]. In electromagnetic interference (EMI) shielding the radiations being shielded by absorption, reflection, or numerous reflections. This phenomenon is also known as microwave absorption and the absorption method is significantly more efficient and effective than the other processes. Microwave sensing and communication are also very essential in the military and civil industries, resulting in an increased interest in using high-efficiency electromagnetic (EM) wave absorbers for stealthy and shielding technologies. The good electromagnetic wave absorption materials should have a high absorption efficiency, a broad absorbing bandwidth, high resistivity, low density, and a reasonable cost [52,53].

The materials such as metallic oxides , metal particles , carbon materials ,ferrites, and conductive polymers are excellent EM wave absorbers due to their high absorption efficiency and unique material features. These shielding material includes Absorption, reflection, and transmission coefficients and the total shielding efficiency of the material is the sum of these three processes which may be expressed as [54]

$$SE = SE(A) + SE(R) + SE(T).$$

Where the coefficients are expressed as

SE(A) (dB) = 10log(1-R/T)

SE(R) (dB) = 10log (1/T)

SE(T) (dB) = 10log (1/1-R)

Amongs these materials, M-type barium ferrite ($BaFe_{12}O_{19}$) is very useful in practical applications due to its ease of manufacture, nontoxicity, and exceptionally low cost. Because of its extraordinary magnetic loss caused by natural resonance, ferrite serves as a microwave absorber [55]. The natural resonance frequency of $BaFe_{12}O_{19}$ is, however, reported to be as high as 43.5 GHz [56].

Therefore, the natural resonance frequency should be modified to the lower range in order to produce absorption within 2–18 GHz. Since the magnetic anisotropy (H_A), which is produced by the exchange-coupling of the Fe^{3+} ions in the lattice, directly correlates to the natural resonance frequency of ferrites . If non-magnetic or weaker magnetic ions are used in place of the Fe^{3+} ions, H_A will decrease. The magnetic anisotropy (H_A), may be reduced more if the Fe^{3+} ions are replaced. Therefore, after the natural resonance with the Fe^{3+} ions being replaced, the reflection loss (R_L) peaks may move to a lower frequency range. Microwave absorption efficiency of the material can also be enhanced by improving the complex permittivity of the material . Barrium ferrite co-doped with Zr^{4+} -Ni^{2+} [$BaFe_{12-2x}(ZrNi)_x O_{19}$],

were synthesized by Zhang et.al and further sintered in Ar observe that these ferrites exhibit strong absorption of −53.9 dB and broad bandwidth of about 6.9 GHz within the frequency range of 2–18 GHz.[57].

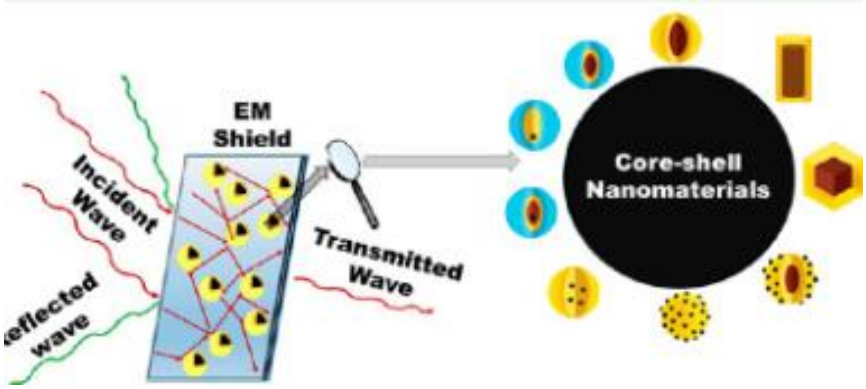

Figure 7. EMI Shielding adopted from[58]

Microwave absorption in Cr^{3+} doped M-type Sr hexaferrite in X-band was investigated by K. Praveena et al. As the quantity of Cr^3 increased, the reflection coefficient increased from -16 to -

33 dB. All doped compositions showed more than -20 dB reflection coefficient from 9.7 to 11 GHz, and the linear rise in absorption was visible with doping from x = 0.0 to 0.9 [59].

2. Biomedical Application (Magnetic Hyperthermia)

Cancer has emerged as a major public health concern, as it is the world's second biggest cause of death, with rising mortality rates (an expected 9.6 million deaths in 2018)[60]. Cancer is a stage of an internal disorder when some of the body cells grow uncontrollably to create complex tissue structures known as tumours. Significant advancements in the field of oncology have been made possible by a variety of therapeutic techniques, including surgery, radiation, chemotherapy, immunotherapy, and gene therapy. The majority of these techniques are linked to a number of serious problems that may have negative clinical consequences on healthy normal cells close to the target area [61]. Beside these Nanocarrier based drug delivery is gaining lot of attention due to the size of nanoparticles (NPs) and specific localization to the target site [62].

Hyperthermia (HPT) thermal therapy, is a promising alternative cancer treatment method in which heat produced from magnetic nanoparticles (MNPs) under a radio frequency magnetic field is used to kill malignant cells. These MNPs are small enough to overcome biological barriers and particularly target tumour locations, and their therapeutic efficacy can be increased by altering their size, shape, and surface properties.

Materials having highly saturated magnetization, such as cobalt , iron, , nickel, manganese, zinc, magnesium, gadolinium, and oxides ($CoFe_2O_4$, $ZnFe_2O_4$, $NiFe_2O_4$, $MnFe_2O_4$, $CuFe_2O_4$, ,Gd-doped Zn-Mn, Zn-Mn-doped iron and Fe-doped Au) or iron oxides (such as magnetite and maghemite) are some of the explored MNPs for MHT due to their effective magnetic properties [63,64]. Pure metals have the highest saturation magnetization, but they are also the most oxidation-sensitive and poisonous materials [65].Therefore, such pure metal nanoparticles are not suitable for biomedical applications without suitable surface treatment. Single domain magnetite and maghemite nanoparticles with diameters ranging from 5 to 20 nm are promising candidates for biomedical applications such as magnetic hyperthermia, owing primarily to their biocompatibility [66]. However, The main problem with these material is that their magnetic characteristics, and thus heating behaviour, are difficult to manage. The specific absorption rate (SAR), which measures the amount of heat lost per unit mass of magnetic material, can be used to measure the heating of magnetic nanoparticles in RF magnetic fields. This is determined by multiplying the material's hysteresis loop area by the frequency of the applied ac magnetic field. The specific loop area for randomly oriented magnetic nanoparticles is given by $A = \pi\mu_o^2 H^2_{max} M^2_S V.\ \omega\tau/\ 3\kappa_B T.\ (1+\omega^2\tau^2)$, where μo is vacuum permeability, M_S is saturation magnetization, V is the volume of magnetic nanoparticles , k_B is the Boltzmann constant, T is absolute temperature, and τ is the Néel Brown relaxation time expressed as $\tau = \tau_o \exp(K_{eff} V)/k_B T$, here K_{eff} is the effective anisotropy constant. Since A depends on magnetic parameters (effective anisotropy, saturation magnetization and particle volume) and also depends on experimental parameters like frequency, temperature, field and amplitude so it's very difficult to predict the response of the specific absorption rate (SAR) .In order to alter intrinsic magnetic properties like saturation magnetization and effective anisotropy doping with appropriate

elements (such as Co ,Ni, , Mn in $ZnFe_2O_4$ and Sr, Ag, Ba in LaMnO3) and creating composites out of magnetically hard and soft materials are used[67].

Strontium hexaferrite, $SrFe_{12}O_{19}$, is of relevance in this context because it has a very significant uniaxial anisotropy = 3.8 105 J/m3 at 300 K [68]. The substitution of tetravalent cations such as Ti^{+4}, Ir^{+4}, Sn^{+4} together with divalent cations such as Zn^{+2}, Mn^{+2}, Co^{+2} into the Fe^{3+} sites might result in a gradual decrease in magnetocrystalline anisotropy and coercivity. The magnetic properties of hard/soft $SrFe_{12}O_{19}$ /$ZnFe_2O_4$, $SrFe_{12}O_{19}$ /$NiFe_2O_4$ /ZnFe2 O 4 , and $SrFe_{12}O_{19}$ /γ-Fe_2O_3 composites suggest that exchange coupling between these hard/ soft phases strongly influences the magnetization andcoercivity. Jose et.al investigated the structural and magnetic properties of strontium hexaferrite based composite materials (soft $MgFe_2O_4$ and hard $SrFe_{12}O_{19}$) phases along with nonmagnetic (ZrO_2) phase. Their heating ability was evaluated in a 214 kHz RF field with an amplitude of 22 Oe. The result indicate that composites of $MgFe_2O_4$/ $SrFe_{12}O_{19}$ /ZrO_2 are attractive candidates for magnetic hyperthermia[69]

Hoopes et al. created ferromagnetic, dextran-coated nanoparticles (100 nm) and found that they supplied heat to tumour cells while having no negative effects on surrounding cells in vitro and in vivo. The findings revealed that magnetic hyperthermic therapy considerably slowed tumour regrowth and that co-treatment with radiotherapy or chemotherapy had further effects[68].

Majeed et al. synthesis tunable-shell-thickness iron oxide nanospheres (15–35 nm) and treated them with silica. MNPs showed a higher specific absorption rate and more successfully eliminated cancer cells in vitro as compared to bare nanoparticles [70].

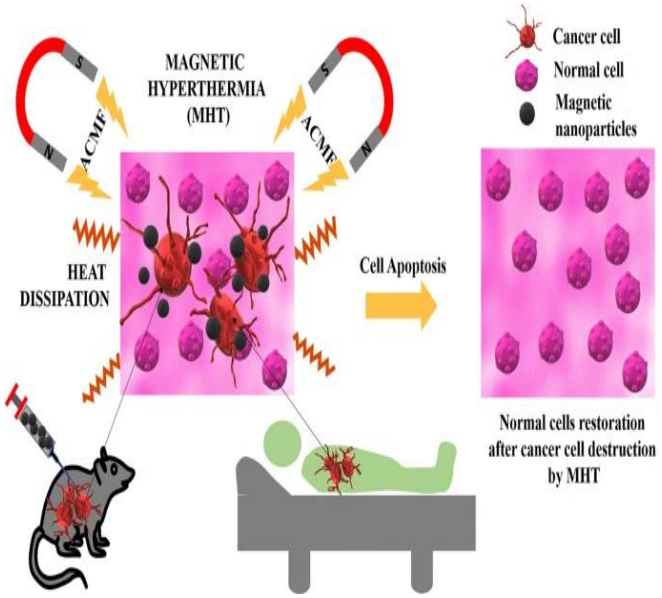

Figure 8 : Pictorial representation of magnetic nanoparticles and cancer cell destruction by MHT adoped from [71]

Liu et al. synthesised nanoflowers, a new class of $Fe_{0.6}Mn_{0.4}O$ nanoparticles, and used them to cure cancer cells in vitro. At a modest dose of 50 g mL1, the synthesised nanoparticles efficiently heated and prevented tumour growth in vivo without damaging adjacent healthy cells [72].

Gaweda et.al uses barium ferrite ($BaFe_{12}O_{19}$) nanoparticles as multifunctional carriers for ^{223}Ra radionuclide for magnetic hyperthermia. [73].

3.Magnetic Recording

In this day and age of information and the Internet, improved high-density memory devices are necessary in many technological disciplines[74]. RAM (resistive random-access memory) Magnetic random-access memory [75,76], phase-change memory and ferroelectric memory [77,78] have all been proposed as next-generation memory technologies. Ferrites have been among the most relevant magnetic materials and have applications in the disciplines of magnetic recording media. A study in the scientific literature shows that altering the stacking sequence of metal rich ferrites can significantly improve the intrinsic properties, especially magnetic and electrical properties. M-type Hexaferrites (Sr, Ba, Ca, Pb) have been known for their high saturation magnetization, resistance, electrical resistivity, and low dielectric losses. It has been found that the synthesis process as well as doping have a significant impact on the intrinsic properties of hexaferrites. In M-type hexagonal ferrites, there are four Fe^{3+} ions with uncompensated upward spins, resulting in a total magnetic moment of 20 mB per formula unit. At lower substitution levels, Ni^{2+} replaces Fe^{3+} from the 4f2 site (downward electronic spin) while at higher substitution levels, Ni^{2+} replaces Fe^{3+} from the 12k crystallographic site (upward electronic spin). In the presence of Ni^{2+}, saturation magnetization and remanence values increase because the unpaired electrons have upward spin instead of the downward spin site (4f2). Consequently, both Ms and Mr values increase. Dy^{3+} replacing Sr^{2+} changes the symmetry surrounding the 2b site, enhancing the hyperfine interactions at the 2b and 12k sites. This might increase the super exchanges interactions and hence the net magnetization. Ashiq et.al report the increase in coercivity (Hc) from 107 to 177 kA /m with increase in Dy-Ni concentration. The increase in coercivity give rise the production of ferrous ions at the 2a lattice site which boosts the hyperfine interactions at the 2b and 12k sites. Increased hyperfine interactions increase magne- tocrystalline anisotropy, resulting in increased coercivity. The increased remanence, saturation magnetization, and coerciveness of the produced materials indicate that they can be useful for perpendicular magnetic recording media [79].

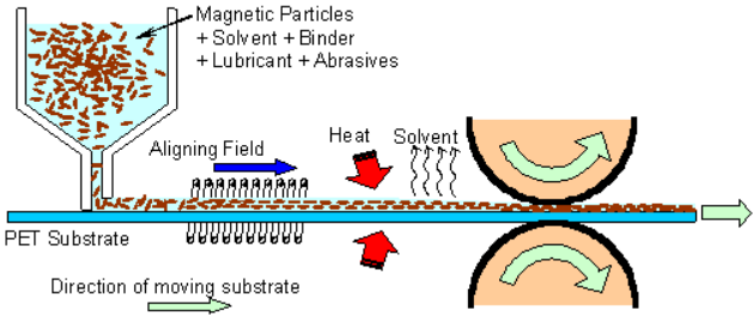

Figure 9: The processing route for particulate magnetic tape adopted from [82]

4.High Frequency Electronic Devices

Communication technology plays a crucial role in the development and progress across the world. The wide range of applications being found for broadband and high frequency of electronic components. Low Temperature Cofired Ceramics and Ferrites (LTCC) have emerged as an attractive technology in recent years for electronic substrates and components that are small and light. It provide high-speed functionality for portable electronic devices like cell phones, personal digital assistants, and personal computers, used for wireless voice and data communication in quickly developing mobile network systems. Due to their increased multifunctionality, sub-miniaturization, higher performances, frequency and excellent reliability, It was required to have a passive components, especially the chip inductors, design to work in high frequency region with very large inductance.[80,81].

Li et.al used ZnTi substituted hexaferrite ($BaFe_{12}O_{19}$) as the high frequency ferrites for the fabrication of chip inductors by LTCC technology. From the spectrum, it was observed that the permeability(u') is relatively stable with the frequency, but varied quickly when the frequency reached to 500MHz. Since the the cut-off frequencies of the ferrite lies beyond 500MHz, which indicates the possibility of high frequency application of ferrites figure below shows the internal multilayer structure the inductors. The permeability of the materials was calculated to be 13.5 and the cut-off frequency at 800MHz [82].

Figure 10: Mutilayer structure of inductor adoped from []

Tsutaoka et.al. study the permeability and permittivity spectra of sintered polycrystalline Ba ferrites, $BaFe_{12-x}(Ti\ Co)_xO_{19}$ with (x=0 to 5) from RF to microwave band up to 10 GHz. The complex permeability spectra of $BaFe_{12-x}(Ti\ Co)_xO_{19}$ at (x=3) shows higher permeability about 16. Recently, it has been reported that relatively high magnetic permeability of compound can be used for the high frequency multilayer inductor [83].

■ REFERENCES

[1] Jeevanandam, J.; Barhoum, A.; Chan, Y. S.; Dufresne, A.;Danquah, M. K. Review on nanoparticles and nanostructured materials: history, sources, toxicity and regulations. Beilstein J. Nanotechnol. 2018, 9 (1), 1050−1074

[2] R. Valenzuela, Novel applications of ferrites, Physiother. Res. Int. 2012 (2012)

[3]V. Tsakaloudi, V.T. Zaspalis, A new Mn-Zn ferrite for high-speed data transmission applications in telecommunication networks, J. Magn. Magn Mater. 310 (2007) 2540–2542, https://doi.org/10.1016/j.jmmm.2006.11.143.

[4] T. Fujiwara, Magnetic properties and recording CHARACTERRISTICS OF barium ferrite media, IEEE Trans. Magn. 23 (1987) 3125–3130.

[5] M.P. Sharrock, L.W. Carlson, The application of barium ferrite particles in advanced recording media, IEEE Trans. Magn. 31 (1995) 2871–2876, https://doi. org/10.1109/20.490177

[8] H.N. Abdelhamid, H.F. Wu, Facile synthesis of nano silver ferrite (AgFeO2)

modified with chitosan applied for biothiol separation, Mater. Sci. Eng. C 45 (2014) 438–445, https://doi.org/10.1016/j.msec.2014.08.071.

[9] Z. Karimi, L. Karimi, H. Shokrollahi, Nano-magnetic particles used in biomedicine: core and coating materials, Mater. Sci. Eng. C 33 (2013) 2465–2475, https://doi.org/10.1016/j.msec.2013.01.045.

[11] J.J. Went, G.W. Rathenau, E.W. Gorter, G.W. van Oosterhout, Hexagonal iron-oxide

compounds as permanent-magnet materials, Phys. Rev. 86 (1952) 424–425.

[12] R.C . Pullar, A.K. Bhattacharya, jmmm 300: 490-499(2006).

[13] X. Sui, M.h. Kryder, B.Y . Wong, D.E. Laughlin, IEEE trans. 29: 3751(1993)

[14] J. F. Nye, Physical Properties of Crystals: Their Representation by

Tensors and Matrices , Clarendon Press , Oxford, 1985 .

[15] N. A. Spaldin, M. Fiebig, Science 2005 , 309 , 391 .

[16] C.-B. Eom, S. Trolier-McKinstry, MRS Bull. 2012 , 37 , 1007 .

[17] H. Schmid, Int. J. Magn. 1973 , 4 , 337

[18] L. D. Landau and E. M. Lifshitz, Electrodynamics of continuous media (Fizmatgiz, Moscow, (1959).

[19] I. E. Dzyaloshinskii, Sov. Phys. JETP 10, 628 (1959).

[20] D. N. Astrov, Sov. Phys. JETP 11, 708 (1609).

[21] Dennis CL, Borges RP, Buda LD, Ebels U, Gregg JF, Hehn M, Jouguelet E, Ounadjela K, Petej I, Prejbeanu IL, Thornton MJ (2002) The defining lengthscales of mesomagnetism: a review. J Phys 14:11

[22] Lone et al. Nanoscale Research Letters (2019) 14:142.

[23] M.A. Almessiere, Y. Slimani, H. Güngünes¸, V.G. Kostishyn, S.V. Trukhanov, A. V. Trukhanov, A. Baykal, Impact of Eu3+ ion substitution on structural, magnetic and microwave traits of Ni–Cu–Zn spinel ferrites, Ceram. Int. 46 (2020)

[24] Aminoff G. Geol Foren Stockh Forh 1925;47:283.

[25] Adelskold V. Arkiv Kemi Min Geol 1938;12a:1.

[26] Wijn HPJ. Nature 1952;170:707.

[27] Braun PB. Nature 1952;170:708

[28]Monika Chandel, Virender Pratap Singh, Rohit Jasrotia, Kirti Singha, Rajesh Kumar. A review on structural, electrical and magnetic properties of Y-type hexaferrites synthesized by different techniques for antenna applications and microwave absorbing characteristic materials[J]. AIMS Materials Science, 2020, 7(3): 244-268.

[29] Pullar, R. C. (2012). Hexagonal Ferrites: A Review of the Synthesis, Properties and

Applications of Hexaferrite Ceramics. Prog. Mater. Sci. 57 (7), 1191–1334. Sep.2012. doi:10.1016/J.PMATSCI.2012.04.001

[30] Van Arkel AE, Verwey EJW, Van Bruggen MG. Rev Trv Chim 1936;55:331.

[31] International Centre for Diffraction Data, Newton Square, PA, USA PDF No. 84-1531 (SrFe 12O 19), 84-757 (BaFe 12O 19), 84-2046 (PbFe 12O 19).

[32] Li Z, Gao F. Can J Chem 2011;89:573.

[33] H. Kojima, in Ferromagnetic Materials, edited by E. P. Wohlfarth (North-Holland, Amsterdam,1982), p. 305.

[34] E. W. Gorter, Proc. IEEE B 104, 255 (1957).

[35] A. Moitra, S. Kim, S.-G. Kim, S.C. Erwin, Y.-K. Hong, J. Park, Defect formation

energy and magnetic properties of aluminum-substituted M-type barium hexaferrite, Computational Condensed Matter (2014)

[36] A Cocherdt: J. Appl .Phys.,34,1273(1963)

[37] M.M. Hessien, M.M. Rashad, M.S. Hassan, K. El-Barawy, Synthesis and magnetic

properties of strontium hexaferrite from celestite ore, J. Alloys Compd. 476 (2009) 373–378.

[38] A.M. Bolarín-Miró, F. Sánchez-De Jesús, C.A. Cortés-Escobedo, S. Díaz-De la Torre, R. Valenzuela, Synthesis of M-type SrFe12O19 by mechanosynthesis assisted by spark plasma sintering, J. Alloys Compd. 643 (2015) S226–S230.

[39] I. Novrita, Dedi, M. Azwar, Investigation of Grain exchange interaction effects on the magnetic properties of strontium hexaferrite magnets, KnE Eng. 4 (2019).

[40] T. Schmidt, D. Seifert, J. Töpfer, Phase formation and saturation magnetization of La-Zn-substituted M-type strontium ferrites, J. Magn. Magn. Mater. 508 (2020) 166887.

[41]Chen, D.-M., Li, Y.-X., Han, L.-K., Long, C., and Zhang, H.-W. (2016). Perpendicularly Oriented Barium Ferrite Thin Films with Low Microwave Loss, Prepared by Pulsed Laser Deposition. Chin. Phys. B 25, 068403–068406

[42] Kimura, T. (2012). Magnetoelectric Hexaferrites. Annu. Rev. Condens. Matter

Phys. 3 (1), 93–110. doi:10.1146/annurev-conmatphys-020911-125101

[43] Khojaste khoo M., Kameli P.Structure and Magnetization of Strontium Hexaferrite (SrFe12O19) Films Prepared by Pulsed Laser Deposition ;Frontiers in Materials 8 (2021).

[44] M. Effendi, E. Nugraha, W. Tri Cahyanto, W. Widanarto, The effects of milling time on structure, magnetic properties and microwave absorption capability of strontium lanthanum ferrite compounds, J. Phys. Conf. Ser. 1494 (2020) 012042.

[45] J. Mohammed, T.T.C. Trudel, H.Y. Hafeez, D. Basandrai, G.R. Bhadu, S.K. Godara,

S.B. Narang, A.K. Srivastava, Design of nano-sized Pr3+–Co2+-substituted M-type strontium hexaferrites for optical sensing and electromagnetic interference (EMI) shielding in Ku band, Appl. Phys. A 125 (2019) 251.

[46] Z. Saeed, B. Azhdar, A novel method for synthesizing narrow particle size distribution of holmium–doped strontium hexaferrite by sol-gel auto-combustion, Mater. Res Express 7 (2020) 045006.

[47] T. Jayakumar, C.R. Raja, S. Arumugam, Structural, magnetic and optical analysis of Pb2+- and Ce3+-doped strontium hexaferrite, J. Supercond. Nov. Magn. 33 (2020) 2451–2458.

[48] M. Hassan, G.A. Ashraf, B. Zhang, Y. He, G. Shen, S. Hu, Energy-efficient de-

gradation of antibiotics in microbial electro-Fenton system catalysed by M-type

strontium hexaferrite nanoparticles, Chem. Eng. J. 380 (2020) 122483.

[49] International Centre for Diffraction Data, Newton Square, PA, USA PDF No. 84-1531 (SrFe12O19), 84-757 (BaFe 12O 19), 84-2046 (PbFe12O19).

[50] Lisnevskaya IV, Aleksandrova IA. Gel Synthesis of Hexaferrites $Pb_{1-x}La_xFe_{12-x}Zn_xO_{19}$ and Properties of Multiferroic Composite Ceramics PZT–$Pb_{1-x}La_xFe_{12-x}Zn_xO_{19}$. Nanomaterials. 2020; 10(9):1630. https://doi.org/10.3390/nano10091630

[51] P. Saini, V. Choudhary, B.P. Singh, R.B. Mathur, S.K. Dhawan, Polyaniline – MWCNT nanocomposites for microwave absorption and EMI shielding, Mater. Chem. Phys. 113 (2009) 919–926, https://doi.org/10.1016/j.matchemphys.2008.08.065.

[52] J.Z. He, X.X. Wang, Y.L. Zhang, M.S. Cao, Small magnetic nanoparticles decorating reduced graphene oxides to tune the electromagnetic attenuation capacity, J. Mater. Chem. C. 4 (2016) 7130–7140, https://doi.org/10.1039/c6tc02020h.

[53] X.F. Zhang, X.L. Dong, H. Huang, Y.Y. Liu, W.N. Wang, Microwave absorption properties of the carbon-coated nickel nanocapsules, Appl. Phys. Lett. (2006), 053115, https://doi.org/10.1063/1.2236965, 1–4.

[54] D. Yuping, L. Shunhua, G. Hongtao, Investigation of electrical conductivity and

electromagnetic shielding effectiveness of polyaniline cuping, Duanomposite, Sci.

Technol. Adv. Mater. 6 (2005) 513–518, https://doi.org/10.1016/j.

stam.2005.01.002, 6

[55] C.Y. Liu, Y.J. Zhang, Y. Tang, Z.R. Wang, H.C. Tang, Y. Ou, L. Yu, N. Ma, P.Y. Du,

Excellent absorption properties of BaFe12-x Nb x O19 controlled by multi-resonance permeability, enhanced permittivity, and the order of matching thickness, Phys.Chem. Chem. Phys. 19 (2017) 21893–21903.

[56] A.V. Trukhanov, S.V. Trukhanov, L.V. Panina, V.G. Kostishyn, D.N. Chitanov, I.S. Kazakevich, A.V. Trukhanov, V.A. Turchenko, Strong corelation between magnetic and electrical subsystems in diamagnetically substituted hexaferrites ceramics, Ceram. Int. 43 (2017) 5635–5641.

[57] Y. Zhang, et al. Journal of Magnetism and Magnetic Materials 494 (2020) 165828

[58] Yudhajit Bhattacharjee and Suryasarathi Bose Core−Shell Nanomaterials for Microwave Absorption and Electromagnetic Interference Shielding: A Review ACS Appl. Nano Mater. 2021, 4, 2, 949–972Publication Date:February 11, 2021https://doi.org/10.1021/acsanm.1c00278

[59] K. Praveena, K. Sadhana, H.L. Liu, M. Bououdina, Microwave absorption studies of magnetic sublattices in microwave sintered Cr3þ doped SrFe12O19, J. Magn. Magn Mater. 426 (2017) 604e614.

[60]Gonzales-Weimuller M, Zeisberger M, Krishnan KM (2009) Size dependant heating rates of iron oxide nanoparticles for magnetic fluid hyperthermia. J Magn Magn Mater 321:1947–1950

[61] Liauw SL, Connell PP, Weichselbaum RR (2013) New paradigms and future challenges in radiation oncology: an update of biological targets and technology. Sci Transl Med 5:173sr2

[62] Kauffman KJ, Dorkin JR, Yang JH, Heartlein MW, Derosa F, Mir FF, Fenton OS, Anderson DG (2015) Optimization of lipid nanoparticle formulations for mRNA delivery in vivo with fractional factorial and definitive screening designs. Nano Lett 15:7300–7306

[63] Sharifi I, Shokrollahi H, Amiri S (2012) Ferrite-based magnetic nanofluids used in hyperthermia applications. J Magn Magn Mater 324:903–915

[64] Abenojar EC, Wickramasinghe S, Bas-Concepcion J, Samia ACS (2016) Structural effects on the magnetic hyperthermia properties of iron oxide nanoparticles. Prog Nat Sci Mater Int 26:440–448

[65] L. A. Harris, Ph.D. Thesis, Virginia Polytechnic Institute and State University (2002).

[66] Q. A. Pankhurst, J. Connolly, S. K. Jones, J. Dobson, J. Phys. D: Appl. Phys. 36 (2003), R167

[67] Amin Ur Rashid, Paul Southern, Jawwad A. Darr, Saifullah Awan, Sadia Manzoor, Strontium Hexaferrite (SrFe 12 O19) Based Composites for Hyperthermia Applications, Journal of Magnetism and Magnetic Materials, http://dx.doi.org/10.1016/j.jmmm.2013.05.048

[68] Hoopes PJ, Tate JA, Ogden JA, Strawbridge RR, Fiering SN, Petryk AA, Barry S, Chinn P, Foreman A (2009) Assessment of intratumor non antibody directed iron oxide nanoparticle hyperthermia cancer therapy and antibody directed IONP uptake in murine and human cells. Proc SPIE Int Soc Opt Eng 23:7181:71810P. https://doi.org/10.1117/12.812056

[69] Jose et.al; Magnetic nanoparticles for hyperthermia in cancer treatment: Environmental Science and Pollution Research (2019). https://doi.org/10.1007/s11356-019-07231-2

[70] Majeed J, Pradhan L, Ningthoujam RS, Vatsa RK, Bahadur D, Tyagi AK (2014) Enhanced specific absorption rate in silanol functionalized Fe3O4 core–shell nanoparticles: study of Fe leaching in Fe3O4 and hyperthermia in L929 and HeLa cells. Colloids Surfaces B Biointerfaces 122:396–403. https://doi.org/10.1016/j.colsurfb.2014.07.019

[71] Rajan, A., Sahu, N.K. Review on magnetic nanoparticle-mediated hyperthermia for cancer therapy. J Nanopart Res 22, 319 (2020). https://doi.org/10.1007/s11051-020-05045-9

[72] Liu XL, Ng CT, Chandrasekharan P, Yang HT, Zhao LY, Peng E, Zhang H (2016) Synthesis of ferromagnetic Fe0. 6Mn0. 4O nanoflowers as anew class of magnetic theranostic platform for in vivo T1-T2 dual mode magnetic resonance imaging and magnetic hyperthermia therapy. Adv Healthc Mater 5:2092–2104. https://doi.org/10.1002/adhm.201600357

[73] Gawęda, W. (2019). Barium Ferrite Magnetic Nanoparticles Labeled with 223Ra: A New Potential Radiobioconjugate for Targeted Alpha Therapy and Magnetic Hyperthermia. Journal of Medical Imaging and Radiation Sciences, 50(1), S3. doi:10.1016/j.jmir.2019.03.011

[74] R. Waser, M. Aono, Nonoionics-based resistive switching memories, Nat.

Mater. 6 (2007) 833e840.

[75] J. Åkerman, Toward a universal memory, Science 308 (2005) 508e510.

[76] M. Wuttig, N. Yamada, Phase-change materials for rewriteable data storage, Nat. Mater. 6 (2007) 824e832.

[77] V. Garcia, S. Fusil, K. Bouzehouane, S. Enouz-Vedrenne, N.D. Mathur, A. Barthelemy, M. Bibes, Giant tunnel electroresistance for non-destructive

readout of ferroelectric states, Nature 460 (2009) 81e84.

[78] R. Guo, L. You, Y. Zhou, Z. Shiuh Lim, X. Zou, L. Chen, R. Ramesh, J. Wang, Non-volatile memory based on the ferroelectric photovoltaic effect, Nat. Commun.4 (2013) 1e5

[79] Muhammad Naeem Ashiq, Muhammad Javed Iqbal, Muhammad Najam-ul-Haq, Pablo Hernandez Gomez, Ashfaq Mahmood Qureshi,Synthesis, magnetic and dielectric properties of Er–Ni doped Sr-hexaferrite nanomaterials for applications in High density recording media and microwave devices,Journal of Magnetism and Magnetic Materials,Volume 324, Issue 1,2012,Pages 15-19, ISSN 0304-8853, https://doi.org/10.1016/j.jmmm.2011.07.016.

[80] Eun, Ki Chan; Lee, Young Chul; Choi, Byung Gun; Kim,Dae Jun; Park,Chul Soon. “Fully Embedded Low Temperature Co-fired Ceramics (LTCC) Spiral Inductors for L-Band RF System-in-Package (SIP),” IEICE Transactions on Electronics, Vol. E86-C, No 6(2003), pp. 1089-1092.

[81] Heo, Keun; Lim, JuHwan; Mun, JeDo; Hwang, SungWoo.“Characterization and wideband modeling of miniaturized LTCC helical inductors,” IEEE Microwave and Wireless Components Letters, Vol. 17, No 3(2007), pp .160-162.

[82] Yuanxun Li, Yingli Liu, Shengjun Yuan, Huaiwu Zhang, Hai Nie and Jianhong Kang, "The design and fabrication of LTCC chip inductors for high frequency applications based on barium ferrites," 2010 11th International Conference on Electronic Packaging Technology & High Density Packaging, Xi'an, 2010, pp. 906-908, doi: 10.1109/ICEPT.2010.5582663.

[83] Takanori Tsutaoka, Aiko Tsurunaga, Nobuyoshi Koga, Permeability and permittivity spectra of substituted barium Ferrites BaFe12−x(Ti0.5Co0.5)xO19(x=0 to 5),Journal of Magnetism and Magnetic Materials,Volume 399,2016,Pages 64-71,ISSN 0304-8853,https://doi.org/10.1016/j.jmmm.2015.09.032.